Small-Angle X-Ray Scattering Measurements on Rabbit Muscle Glycogen Phosphorylase Dimer *b* and Tetramer *b**

Gerd Puchwein, Otto Kratky, Christian F. Gölker,† and Ernst Helmreich‡

ABSTRACT: A model for muscle glycogen phosphorylase dimer *b* and tetramer *b* in solution was derived from small-angle X-ray scattering measurements. Solutions of phosphorylase dimer *b* in glycero-*P* buffer, pH 7.5, $r/2 = 0.13$ with and without 5′-AMP at 30° appeared to be quite homogeneous, as judged from their sedimentation behavior in the ultracentrifuge. Thus, it was possible to study directly the structure of dimer *b* in solution. Phosphorylase tetramer *b* solutions contained however a significant amount of dimer *b*, even in the presence of 1×10^{-3} M 5′-AMP and 2×10^{-1} M NaF, conditions that favor tetramer *b* formation. It was necessary therefore to develop a method which would allow definition of the structural parameters of one of the components of a paucidisperse mixture. With this method structural parameters of muscle glycogen phosphorylase tetramer *b* in the presence of dimer *b* could be defined. Prism models with the three axes related to each other as A:B:C = 1:1:2 or 1:0.75:1.8 show scattering equivalence with the phosphorylase dimer *b* molecule. In the final model for dimer *b*, the actual relationship of the axes is: A:B:C = 1:0.90:1.78. A tetramer built from two prismatic dimers has the dimensions 55.3 ± 4.9 Å:109.4 ± 2.6 Å:123.2 ± 5.6 Å corresponding to axial ratios of 0.51 ± 0.05:1:1.13 ± 0.06. A tetrameric structure of this kind shows scattering equivalence with a prism model with axial ratios of 1:1:0.5.

The actual form of the phosphorylase protomer may however be represented in part by a prism and in part also by an ellipsoid. The rather large (20%) difference in the particle volume of the real phosphorylase molecule and the model prism was interpreted to suggest a substructure of phosphorylase dimer *b*. This assumption is compatible with the electronmicroscopic data reported previously. The average molecular weight of phosphorylase dimer *b* as determined by small-angle X-ray scattering was 163,000 daltons ± 5%. Different methods used for the determination of the partial specific volume and the extreme sensitivity of molecular weight determinations by X-ray small-angle scattering to changes in the value for the partial specific volume are made responsible for the difference in molecular weights derived from X-ray scattering (163,000) and high-speed sedimentation equilibrium measurements (185,000).

Phosphorylase plays an important role in the regulation of glycogen metabolism in muscle (*cf.* Helmreich and Cori, 1965). It exists in two interconvertible forms: phosphorylase *b* and phosphorylase *a*. In the phosphorylase *b*→*a* conversion, a seryl OH side chain in the phosphorylase protomer *b* is phosphorylated through the action of phosphorylase *b* kinase, ATP, and Mg^{2+}. The reverse reaction, phosphorylase *a*→*b*, is catalyzed by phosphorylase phosphatase. (For further information, see reviews by: Brown and Cori, 1961; Krebs and Fischer, 1962; Fischer and Krebs, 1966; Helmreich, 1969.) Both, the phosphorylated (*a*) and the unphosphorylated (*b*) enzyme can exist as dimers or tetramers or as a mixture of both (Seery *et al.*, 1967). Although, the dimeric state is favored in the case of phosphorylase *b* and the tetrameric state in the case of phosphorylase *a*, at low temperatures and high enzyme concentrations, 5′-AMP readily induces association of dimers *b* to tetramer *b* (Graves *et al.*, 1965; Hedrick *et al.*, 1966; Kastenschmidt *et al.*, 1968a,b). Since, however, glycogen, the natural substrate of phosphorylase, binds preferentially to the dimeric form, the dimer is the catalytically more active form of the enzyme. This was shown to be the case for rabbit and frog muscle glycogen phosphorylase *a* (Wang *et al.*, 1965; Metzger *et al.*, 1967, 1968; Huang and Graves, 1970).

In the case of muscle phosphorylase *b* there is ample evidence for the role of subunit interactions in the regulation of enzymatic activity (see also: Illingworth *et al.*, 1958; Hedrick *et al.*, 1966; Battell *et al.*, 1968; Chignell *et al.*, 1968; Kastenschmidt *et al.*, 1968a; Shaltiel *et al.*, 1969). But, despite the great interest in subunit enzymes and particularly in muscle phosphorylase, little is as yet known about its structure. Comprehensive data are available on the molecular weights and some hydrodynamic properties of muscle phosphorylase *b* and *a* (*cf.* Seery *et al.*, 1967). Recently, Valentine and Chignell (1968) have proposed on the basis of electron microscopic data that the tetrameric form of muscle glycogen phosphorylase *b* has a rhombic shape. We now report the first results of small-angle X-ray scattering measurements on muscle phosphorylase dimer *b* and tetramer *b* in solution. A major difficulty arose in this study because phosphorylase tetramer *b* (or tetramer *a*) is always to a significant extent dissociated to dimers. Phosphorylase dimer *b* solutions were

* From the Institute for Physical Chemistry, The University of Graz, Graz, Austria (G. P. and O. K.), and the Department of Physiological Chemistry, The University of Wuerzburg, Wuerzburg, West Germany (C. F. G. and E. H.). *Received June 12, 1970.* O. K. acknowledges the support of his research by the Austrian "Fonds für wissenschaftliche Forschung." C. F. G. was a recipient of an EMBO (European Molecular Biology Organization) fellowship. Research in the Department of Physiological Chemistry is supported by grants from the Deutsche Forschungsgemeinschaft, the Stiftung Volkswagenwerk and Bundesministerium für Bildung und Wissenschaft.

† Present address: Farbenfabriken Bayer AG, Wuppertal-Elberfeld, West Germany.

‡ To whom correspondence should be addressed.

homogeneous enough to allow direct X-ray scattering measurements. For the analysis of tetramer *b* solutions, however, an indirect approach had to be chosen. The method used is described in this paper. It allows the differential analysis of the structure of one of the components of a paucidisperse system.

Materials and Methods

Preparation and Activity of the Enzyme. Phosphorylase *b* was prepared from rabbit skeletal muscle according to the method of Fischer and Krebs (1958). The enzyme was recrystallized at least three times prior to use. If necessary, 5′-AMP was removed from the enzyme by treatment with charcoal and/or filtration of the enzyme solution through a short column of Sephadex G-25 equilibrated with buffer (*cf.* Kastenschmidt *et al.*, 1968a). The standard buffer solution was sodium β-glycerophosphate, 50 mM; NaEDTA, 2 mM; β-mercaptoethanol, 10 mM; pH 7.5; $\tau/2 = 0.13$. The higher pH helps to keep the enzyme in the dissociated state (*cf.* Graves *et al.*, 1965). The concentration of phosphorylase *b* was determined by absorption measurements at 280 mμ using a value for $\epsilon_{1\,cm}^{1\%}$ 13.2 (*cf.* Kastenschmidt *et al.*, 1968a). Phosphorylase *b* activity was measured in the direction of glycogen synthesis: glycogen$_n$ + glucose-1-P → glycogen$_{(n+1)}$ + P$_i$. The assay conditions described by Kastenschmidt *et al.* (1968a) were used, except that the pH was 7.5. Initial rates were estimated by drawing tangents to the near linear part of the rate curves. P$_i$ was determined by the method of Fiske and Subbarow (1925). In order to see whether phosphorylase *b* was damaged by X-rays, the activity of the enzyme was determined before and after the X-ray scattering measurements. No significant change was noted. The activity of the enzyme ranged from 44 to 50 μmoles of P$_i$ formed per mg of enzyme per min at 30° under standard assay conditions.

Ultracentrifugal Analyses. Sedimentation velocity measurements were performed with a Spinco Model E analytical ultracentrifuge equipped with schlieren optics. The schlieren diagrams were evaluated with a Leitz microcomparator. The percentage of the components with different sedimentation coefficients in associating-dissociating enzyme solutions was estimated from projections of the enlarged sedimentation patterns on paper. The area under the sedimenting peaks was measured with a planimeter. The sedimentation coefficients were corrected for the difference in viscosity and density of buffer and water at 20°. The experimental conditions and the temperatures used for ultracentrifugal analysis were otherwise identical with the conditions for the small-angle X-ray scattering measurements. All enzyme preparations whose scattering behavior was examined were checked independently in the analytical ultracentrifuge.

Materials. Rabbit liver glycogen was obtained from Merck Co. It was freed from nucleotides as described previously by Helmreich *et al.* (1967). All other reagents were of the highest commerically available purity. Double-distilled water was used throughout.

Small-Angle X-Ray Scattering Measurements. The phosphorylase *b* solution was filled into a Mark capillary placed into a constant-temperature cuvet. The temperature was kept constant to ±0.5°. The measurements were done with a X-ray small-angle camera free from parasitic scattering. The apparatus is described elsewhere (Kratky, 1954, 1958; Kratky and Skala, 1958). The detector was moved automatically across the scattering range with a step-scanning device (Kratky and Kratky, 1964; Leopold, 1965). Radiation was registered by a proportional counter equipped with an pulse height discriminator adjusted to the Cu Kα line. Maximal resolution was limited to about 600 Å. All curves represent results from repeated measurements. Furthermore, the X-ray scattering curves were controlled point by point in order to assure that the protein did not change during the measurements. As long as there was no measurable change in the dimer $\rightleftarrows$ tetramer equilibria changing the protein concentration did not alter the scattering curves. Thus, they were superimposable when corrected by multiplication with a scale factor. It was possible therefore to use for further treatment the mean of several superimposed curves obtained at different enzyme concentrations. The procedure considerably improved the reliability of the measurements. All scattering curves were corrected for their collimation error using the computer program of Heine and Roppert (1962); (see also: Heine, 1963). The scattering curves were monochromatized by elimination of the β line (*cf.* Zipper, 1969). The absolute intensity of the scatter was determined using a calibrated Lupolen sample. The Lupolen sample was calibrated as described previously (Kratky, 1960, 1963, 1964; Kratky and Wawra, 1963; Kratky *et al.*, 1966; Pilz and Kratky, 1967; Pilz, 1969).

Theory

Radius of Gyration. Following correction and normalization to unit concentration (*c* 1), the scattering curves were plotted according to Guinier and Fournet (1955). Radii of gyration (*R*) were calculated from the slopes of the Guinier plots using the tangents to zero angle

$$R = \frac{\lambda}{2\pi}\sqrt{3 \times 2.3\,(-\tan\alpha)}\ [\text{Å}] \qquad (1)$$

λ = wavelength of Cu Kα line = 1.54 Å.

The scattering curve of elongated particles can be split into two factors (Kratky and Porod, 1948; Porod, 1948): the Lorentz factor of the length (I_l) and a cross-section factor (I_s): $I = I_l \times I_s$. The length factor is equal $1/2\theta$. The cross-section factor is therefore $I \times 2\theta$. I is the scatter intensity in pulses per second, and 2θ is the scattering angle in radians. One can then determine from Guinier plots (log $I \times 2\theta$ *vs.* $(2\theta)^2$) the radius of gyration of the cross section (R_S). The radii of gyration of the cross section are determined by eq 2 which is analogous to eq 1.

$$R_S = \frac{\lambda}{2\pi}\sqrt{2 \times 2.3\,(-\tan\alpha)}\ [\text{Å}] \qquad (2)$$

Molecular Weight. Molecular weights (*M*) were determined from the absolute scatter intensities which are defined as the ratio of the scattered intensity I_0 at zero angle, to the intensity of the primary beam. The following equations were used (Kratky *et al.*, 1950; Kratky, 1963, 1964):

$$M = \frac{1}{i_0 N_A}\,\frac{I_0}{c}\,\frac{a^2}{\Sigma P D z_1^2} \qquad (3)$$

TABLE I: State of Aggregation and Range of Phosphorylase *b* and 5′-AMP Concentrations.

Temp (°C)	Phosphorylase *b* (mg/ml)	Additions (M)	$s_{20w} \times 10^{-13}$ (sec)
30	10.00	None	
	5.00	None	8.3
	3.00	None	
30	10.75	1×10^{-3} 5′-AMP	8.3
	5.07	1×10^{-3} 5′-AMP	
	2.56	1×10^{-3} 5′-AMP	
30	10.22	5×10^{-3} 5′-AMP	
	7.14	5×10^{-3} 5′-AMP	
	3.59	5×10^{-3} 5′-AMP	
21	13.65	1×10^{-3} 5′-AMP and 2×10^{-1} NaF	12.0,[a] 8.3[b]
	8.81	1×10^{-3} 5′-AMP and 2×10^{-1} NaF	
	4.40	1×10^{-3} 5′-AMP and 2×10^{-1} NaF	

[a] Major component. [b] Minor component (see text and Figure 4).

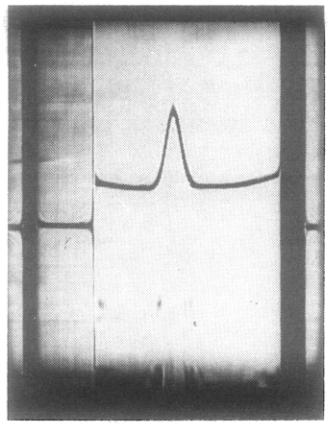

FIGURE 1: Sedimentation of phosphorylase dimer *b* in the absence of 5′-AMP. The concentration of the enzyme was 6.0 mg/ml in glycerophosphate standard buffer, pH 7.5. Temperature was 30°. A 12-mm cell was used. Speed was 59,813 rpm and bar angle 60°; the picture was taken 24 min after reaching full speed; sedimentation was from left to right.

where i_0 = Thomson's constant; N_A = Avogadro's number; I_0 = intensity at zero angle [pulses/sec]; c = concentration [g/cm³]; a = distance of the sample from the plane of registration [cm]; D = sample thickness [cm] ΣP = intensity of the primary beam [pulses/sec]. The term z_1, *i.e.*, the difference in electron density of protein and solvent, in eq 3 is defined by eq 4 where $(\Sigma O/\Sigma A)_P$ = sum of the atomic numbers/

$$z_1 = \left(\frac{\Sigma O}{\Sigma A}\right)_P - \bar{v}\rho_S\left(\frac{\Sigma O}{\Sigma A}\right)_S \quad (4)$$

sum of the atomic weights of the protein, and $(\Sigma O/\Sigma A)_S$ = sum of the atomic numbers/sum of the atomic weights of the solvent, $\bar{v}$ = partial specific volume [cm³/g], and ρ_S = solvent density [g/cm³].

Volume and Degree of Swelling. An invariant term Q of the scattering curves can be obtained according to Porod (1951, 1952). Q is defined by

$$Q = \int_0^\infty \frac{I}{c}(2\theta)^2 \, d(2\theta) \quad (5)$$

Q is derived from the integral of the product of the scattering intensity and the square of the scattering angle over all the scattering angles. For angles $2\theta > 0.05$ radian the scattering curve is proportional $1/(2\theta)$.[4]

From the invariant Q and I_0 the particle volume (V) may be derived according to eq 6. From the values of M,

$$V = 0.291 \frac{I_0/c}{Q} \text{ [Å}^3\text{]}; \; 0.291 = \frac{\lambda^3}{4\pi} \quad (6)$$

$\bar{v}$, and V the internal solvation of the particle could then be calculated. These values are expressed as g of solvent/g of protein.

The partial specific volume ($\bar{v}$) was determined with a precision method developed by Kratky *et al.* (1969) on the same phosphorylase *b* solutions that were used in small-angle X-ray scattering experiments. At 30° this value was in the range studied, independent of changes in protein and 5′-AMP concentrations.

Results

Phosphorylase Dimer b. The range of concentrations of Phosphorylase *b* and 5′-AMP examined is given in Table I.

A serious complication in small-angle X-ray scattering measurements of proteins arises from the fact that most oligomeric proteins in solution exist in equilibrium between monomeric and polymeric forms. The phosphorylase *b* solutions studied at 30° with or without 5′-AMP gave a single homogeneous peak in the ultracentrifuge with a s_{20w} value of 8.3 (see Table I and Figures 1 and 2). This value is representative for the dimeric form of phosphorylase *b* (*cf.* Seery *et al.*, 1967). Thus, judging from these criteria the phosphorylase dimer *b* solutions apparently were homogeneous enough so as to allow a direct analysis of the dimer *b* structure. Curves 1–3 in Figure 3 are Guinier plots for phosphorylase dimer *b*. R for dimer *b* and at 5′-AMP concentrations less than 5×10^{-3} M was 39.6 Å ± 1%. In an experiment with 5×10^{-3} M 5′-AMP the value of R was 40.4 Å ± 1% (see Table II). An admixture of about 3% of tetramer *b* could account for the increase in R. Therefore the value of R = 39.6 Å ± 1 % was used for the following calculations.

5′-AMP promotes transitions from inactive to active states which in the case of muscle phosphorylase *b* have a greater affinity for substrates (Helmreich and Cori, 1964; Madsen, 1964; Kastenschmidt *et al.*, 1968b). A comparison of all the scattering data for phosphorylase dimer *b* in the presence or absence of 1×10^{-3} M 5′-AMP did not reveal any significant change which could be interpreted as the consequence of an AMP-induced conformational transition.

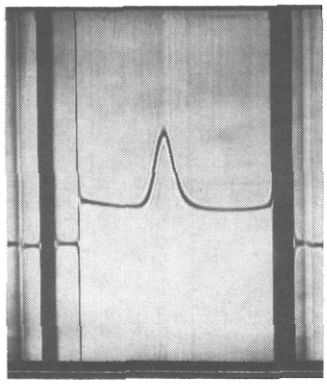

FIGURE 2: Sedimentation of phosphorylase dimer *b* in the presence of 1×10^{-3} M 5′-AMP. The concentration of enzyme was 10.75 mg/ml in glycerophosphate standard buffer, pH 7.5. Temperature was 30°. A 12-mm cell was used. Speed was 56,000 rpm and bar angle 60°. The picture was taken 36 min after reaching full speed; sedimentation was from left to right.

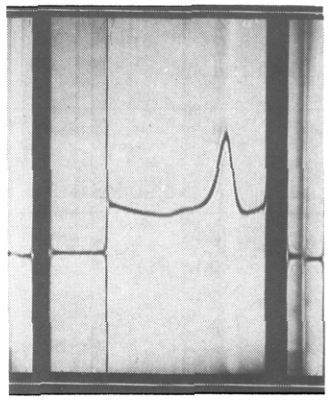

FIGURE 4: Sedimentation of a mixture of phosphorylase dimer *b* and tetramer *b*. The concentration of enzyme was 13.65 mg/ml in glycerophosphate buffer, pH 7.5, containing 1×10^{-3} M 5′-AMP and 2×10^{-1} M NaF; temperature was 21°. A 12-mm cell was used. Speed was 56,000 rpm and bar angle 60°. The picture was taken 42 min after reaching full speed; sedimentation was from left to right.

Phosphorylase Tetramer b. We could not accurately determine directly the scattering curve of the tetrameric form of phosphorylase *b* since under a variety of experimental conditions, not described here, there was always present besides tetramer *b* an appreciable amount of dimer *b*. We finally adopted the conditions described by Sealock and Graves (1967). They have shown that 5′-AMP—especially in the presence of NaF—shifts even at 20° the phosphorylase dimer *b* ⇌ tetramer *b* equilibrium toward the tetrameric form (see Table I, a representative experimental is shown in Figure 4). Under the conditions of the experiment of Sealock and Graves (1967) about 80% of our phosphorylase *b* solution was tetramer *b* and the remainder was dimer *b*. This in only a rough approximation made from area analysis of the sedimenting peaks in the ultracentrifuge. A more accurate determination of the dimer–tetramer distribution in this experiment was made from the absolute intensities of the X-ray scatter. This method indicated 39.4% dimers as shown below.[1]

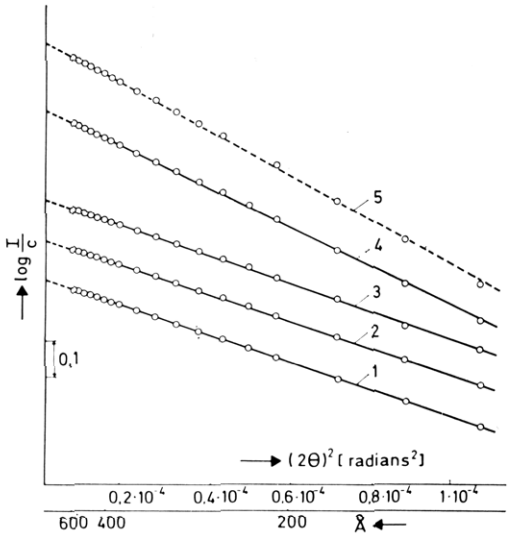

FIGURE 3: Guinier plots of the experimental scattering curves of phosphorylase *b:* curve 1, 30°, no 5′-AMP; curve 2, 30°, 1×10^{-3} M 5′-AMP; curve 3, 30°, 5×10^{-3} M 5′-AMP; curve 4, 21°, 1×10^{-3} M 5′-AMP and 2×10^{-1} M NaF. Curve 5 (dashed line) represents data for tetramer *b*, calculated according to eq 9 (see text). *I*/*c* is the scatter intensity normalized to unit concentration of protein and expressed in pulses per second, 2θ is the scattering angle in radians. The Å scale corresponds to the Bragg values for the scattering angles. The curves are shifted arbitrarily in the direction of the ordinate, in order to present them more clearly.

The dimer–tetramer mixture was treated in the following way. From the scattering curve of a dimer–tetramer mixture of muscle phosphorylase *b* one obtains a median value for *R*, ($\bar{R}$), the radius of gyration (see curve 4, Figure 3). This value is $\bar{R} = 47.8$ Å ± 1%. One obtains a molecular weight average ($\overline{M}_w$). This value is: $\overline{M}_w = (1.606 \pm 0.048) \times M_D$ where M_D is the molecular weight of the dimer in the presence of 1×10^{-3} M 5′-AMP. Thus, the median molecular weight of the mixture ($\overline{M}_w$) represents

$$\overline{M}_w = \frac{M_D c_D + M_T c_T}{c_D + c_T} \tag{7}$$

where the subfixes D and T stand for dimer *b* and tetramer *b*, respectively. Since $M_T = 2\,M_D$ and $c_D + c_T \equiv 1$, one obtains $c_T = 0.606$ and $c_D = 0.394$.

The radius of gyration of the tetramer, R_T, can be derived from

$$\overline{R^2} = \frac{c_D M_D R_D^2 + c_T M_T R_T^2}{c_D M_D + c_T M_T} \tag{8}$$

R_T was 50.2 Å ± 1.5%.

A scattering curve for tetramer *b* is then derived from eq 9.

$$\left[\frac{I(2\theta)}{c}\right] = \frac{c_D}{c_D + c_T}\left[\frac{I(2\theta)}{c}\right]_D + \frac{c_T}{c_D + c_T}\left[\frac{I(2\theta)}{c}\right]_T \tag{9}$$

[1] The large discrepancy between the estimate made from the ultracentrifuge picture and from X-ray scattering points to the difficulties in determining the distribution of components with different molecular weights in associating–dissociating systems.

TABLE II: Molecular Parameters of Phosphorylase Dimer *b* and Tetramer *b*.[a]

Expt	Additions (M)	Temp (°C)	M (daltons)	R (Å)	R_s (Å)	V (Å^3 × 10^{-5})	g of Solvent per g of Protein
I	None	30	160,000 ± 5 %	39.6 ± 1 %	23.6 ± 4 %	3.09 ± 10 %	0.43 ± 30 %
II	1 × 10^{-3} 5′-AMP	30	163,000 ± 5 %	39.6 ± 1 %	24.2 ± 4 %	3.12 ± 10 %	0.42 ± 30 %
III	5 × 10^{-3} 5′-AMP	30	166,000 ± 5 %	40.4 ± 1 %	23.9 ± 4 %	3.27 ± 10 %	0.46 ± 30 %
IV	1 × 10^{-3} 5′-AMP	21	262,000 ± 5 %[b]	47.8 ± 1 %[b]		5.14 ± 10 %	0.45 ± 30 %
	and 2 × 10^{-1} NaF		(326,000 ± 5 %)[c]	(50.2 ± 1.5%)[c]	(~35.9)[c]	(6.52)[c]	(0.47)[c]

[a] Standard deviations from the mean are given in per cent. [b] Values determined experimentally for the dimer *b*–tetramer *b* mixture (see text). [c] Values in parentheses are derived values for tetramer *b* in expt IV (see text and eq 9).

All terms in eq 9 are known with the exception of the term $[I(2\theta)/c]_T$. The derived scattering curve for tetramer *b* is not as accurate as a scattering curve determined by direct measurements would have been. Curve 5 of Figure 3 is the derived scattering curve for tetramer *b*.

Molecular Parameters. Table II contains data for several molecular parameters of muscle phosphorylase dimer *b* and tetramer *b*, including molecular weights.

By small-angle X-ray scattering one obtains an average molecular weight for phosphorylase dimer *b* of M = 163,000 ± 8000 daltons. This value is lower than the value of 185,000 daltons obtained from high-speed sedimentation equilibrium measurements by Seery *et al.* (1967). Seery *et al.* (1967) have determined the partial specific volume ($\bar{v}$) of phosphorylase *b* from the amino acid analysis and the apparent specific volume from density measurements at 20° using a Cahn electrobalance and have obtained a value of $\bar{v}$ = 0.737 ml/g. The value determined by us with a different method was $\bar{v}$ = 0.729 ± 0.04 ml/g (see Theory: Volume and Degree of Swelling). Molecular weight determinations based on X-ray small-angle scattering are exceedingly sensitive to changes in the value for the partial specific volume. A change of 1% in the value for $\bar{v}$ would have changed in this particular case the value for the molecular weight by 6.6%. Thus, the differences in the molecular weights are primarily due to the different values of $\bar{v}$.

The particle volume of the dimer–tetramer mixture as determined from Q and I_0 increases in a parallel fashion with increasing molecular weight. Considering the limitations in the accuracy of the analysis of dimer–tetramer mixtures, it would seem that the degree of swelling for phosphorylase dimer *b* and phosphorylase tetramer *b* is about the same.

Molecular Shape. There are a number of structural models (prisms, cylinders, ellipsoids) that would fit within the limits of the method the scattering curves of the phosphorylase molecule. If, however, molecular symmetry in oligomeric proteins is postulated (Monod *et al.*, 1965), then the number of plausible models becomes greatly restricted. For example, one may assume that in phosphorylase dimer *b* and tetramer *b* two out of three coordinate axes have the same length and that the third axis in tetramer *b* is about twice as long as that in dimer *b*. This implies that symmetry is preserved when two dimers *b* associate to tetramer *b*. It also implies that the overall conformation is preserved in the course of the association reaction. Experimental observations impose further restrictions. (1) The distance L between the centers of the two dimeric units in the tetramer, can be calculated from the radii of gyration for dimer *b* (R_D) and tetramer *b* (R_T) according to eq 10. It thus follows that

$$L = 2 \times \sqrt{R_T^2 - R_D^2} = 61.6 \pm 2.8 \text{ Å} \qquad (10)$$

(2) The radii of gyration for the cross section of the dimer *b* model (R_{SD}) and the tetramer *b* model (R_{ST}) must agree with the experimentally determined values for the corresponding parameters which were derived from the log $(I/c) \times 2\theta/(2\theta)^2$ plots (*cf.* Figure 5 and Table II).

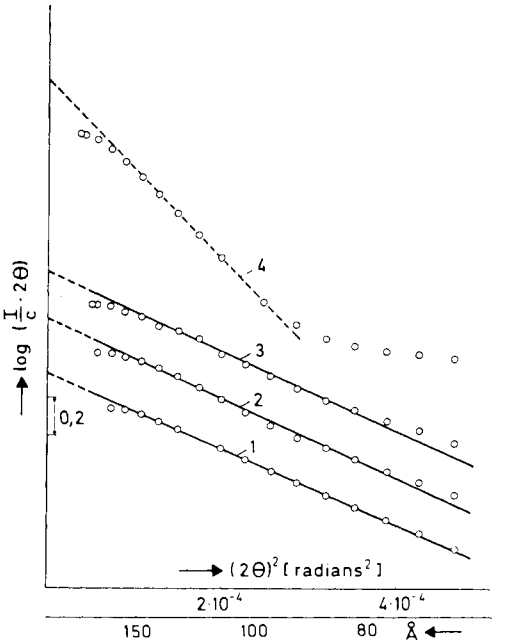

FIGURE 5: Cross-section factors of phosphorylase dimer *b* and tetramer *b*. Conditions and symbols are those given in Figure 3. Curves 1–3 represent dimer *b* and correspond to curves 1–3 of Figure 3 while curve 4 represents tetramer *b* and corresponds to curve 5 of Figure 3.

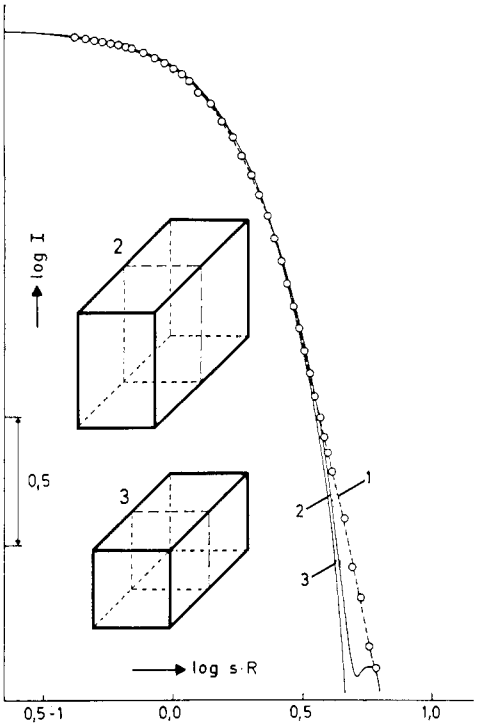

FIGURE 6: Log–log plots of the experimental scattering curve of phosphorylase dimer *b* and the theoretical scattering curves of rectangular prisms: curve 1, experimental scattering curve of phosphorylase dimer *b* at 30°, without 5′-AMP; curve 2, theoretical scattering curve of a rectangular prism with an axial ratio of: 0.75:1:1.8; curve 3, theoretical scattering curve of a rectangular prism with an axial ratio of 1:1:2; $s = (4\pi/\lambda) \sin\theta$; R is the radius of gyration and I is the scatter intensity in arbitrary units.

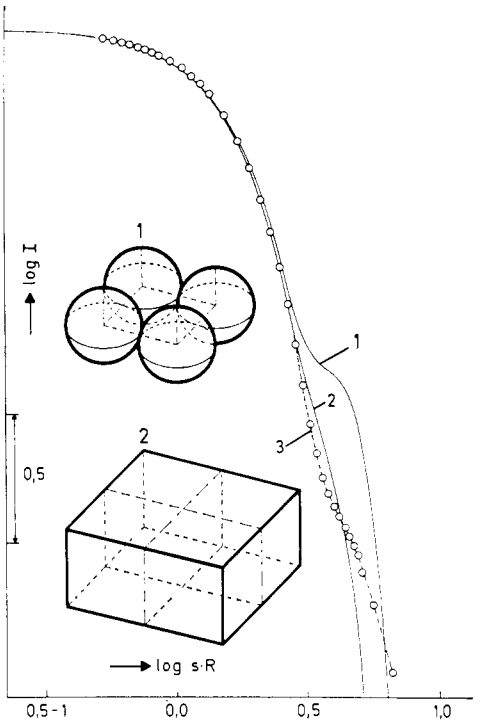

FIGURE 7: Log–log plots of theoretical scattering curves for model structures and the experimental scattering curve of phosphorylase tetramer *b*. Model 1 represents four spheres in a quadratic arrangement. Model 2 represents a rectangular prism with the axial ratio 1:1:0.5. Curves 1 and 2 are theoretical curves for model 1 and 2, respectively. Curve 3 is the scattering curve for tetramer *b* and was determined from eq 9 (see text). Symbols are the same as in Figure 6.

Assuming that the shape of the dimer *b* molecule approximates that of a rectangular prism with the edges *A*, *B*, and *C*, the length *C* can then be calculated according to eq 11.[2] *C*

$$C = \sqrt{12} \times \sqrt{R_D^2 - R_{SD}^2} \qquad (11)$$

was found to be 109.4 ± 2.6 Å if a mean value of 23.9 Å was used for R_{SD}.

The two shorter axes *A* and *B*, are related to the radius of gyration of the cross section (R_{SD}) as shown in eq 12.

$$A^2 + B^2 = 12\, R_{SD}^2 \qquad (12)$$

If one sets, in accordance with the rationale stated above, *A* equal to the distance (*L*) between the two centers of the dimeric subunits in tetramer *b* one obtains for $A:A = L =$ 61.6 ± 2.8 Å. B is readily derived by eq 12 and was found to be 55.3 ± 4.9 Å. The three axes are then related to each other as $A:B:C = 1:0.90 \pm 0.09:1.78 \pm 0.09$.

A comparison of the experimental curve for dimer *b* with scattering curves of model prisms with axial ratios of 1:0.75:1.8 and of 1:1:2—all with the same radii of gyration as dimer *b*—shows that the two theoretical curves and the experimental curve agree reasonably well (*cf.* Figure 6). The axial ratios of the model which we have finally chosen are in the above range.

A prismatic model of a tetramer built from two prismatic dimers has the dimensions 55.3 ± 4.9 Å:109.4 ± 2.6 Å: 123.2 ± 5.6 Å corresponding to axial ratios of 0.51 ± 0.05: 1:1.13 ± 0.06. In Figure 7 are compared scattering curves for tetramer *b* and for a prismatic model with an axial ratio of 0.5:1:1. The radius of gyration of the cross section of this model is R_{ST} = 35.4 Å. This value may be compared with the value of R_{ST} = 35.9 Å calculated for tetramer *b* according to eq 2. The close agreement of the two values is, however, not as convincing as it looks, since it is not possible to determine the radius of gyration of the cross section of so short a particle from a log $(I/c) \times 2\theta/(2\theta)^2$ plot with sufficient accuracy (see Figure 5, curve 4).

The volumes calculated for these prismatic models are about 20% greater than the values determined for the phosphorylase molecule according to eq 6. It is not likely that this rather large deviation results alone from experimental inaccuracies in the determination of the invariant *Q* from the scattering curves. It probably reflects the deviation of the true shape of the phosphorylase molecule from the ideal shape of a prism (see Discussion).

Discussion

The main purpose of this study was to find plausible models for oligomeric proteins that exist in solution as mixtures

[2] The theory for the derivations may be found in the paper of Mittelbach (1964).

of monomeric and polymeric forms. The approach described above, in conjunction with ultracentrifugal analysis, made it possible to outline, at least in rough approximation the structural parameters of an associating–dissociating oligomeric protein. Since many regulatory proteins are associating–dissociating oligomers, the results obtained with the small-angle X-ray scattering method and skeletal muscle glycogen phosphorylase *b* might be of more general interest.

The dimensions of the model structure (55.3:61.6:109.4 Å) that fit the experimental scattering curves of phosphorylase dimer *b* and the dimensions (55:65:110 Å) calculated by Chignell *et al.* (1968) from electron-diffraction patterns of phosphorylase *b* crystals fixed in glutaraldehyde agree well. It is obvious, that a rectangular prism can only be a very rough approximation of the actual form of the phosphorylase *b* protein. It would have been desirable to test other models with respect to their scattering equivalence with phosphorylase *b*, but computer programs for the calculation of models made of several cylinders are not yet available. Thus we could not compare for instance a model made of two elliptic cylinders with the scattering curve of phosphorylase tetramer *b*. This would have been interesting because theoretical scattering curves of elliptic cylinders, not shown here, fit the experimental curve of dimer *b* just as well as the prisms described above and in Figure 6. Our calculations indicate, however, that the dimensions of elliptic cylinders and of rectangular prisms are not much different. Since we had access to a computer program for calculating scattering curves for models made of ellipsoids in arbitrary arrangements (Pilz *et al.*, 1970) we built models, assuming that the protomers of dimer *b* and tetramer *b* are stacked ellipsoids (see Figures 7 and 8). These models, however, did fit much less closely the experimental scattering curves than did the prismatic models (compare Figures 6–8). Moreover, such structures have about 10% greater overall dimensions than a prism with the same radius of gyration.

It may be noted from Figures 6 and 7, that experimental curves for phosphorylase and theoretical scattering curves calculated for a model prism deviate to some extent at the outer parts of the curves. Although in the case of the phosphorylase protein, the experimental inaccuracy was larger for the determination of the outer parts of the scattering curves, there is a more likely explanation for these discrepancies: The deviations of theoretical from experimental curves may again reflect differences in the shapes of the real molecule and the model. This is supported by a comparison of the theoretical curves for prismatic and ellipsoid models which showed that substructures in a particle have a much greater influence on the shape of the outer than on the inner parts of the scattering curves (see Figures 6–8). Thus, the protomer of phosphorylase *b* might have a shape in between that of a prism and an ellipsoid. The assumption that phosphorylase dimer *b* has a substructure is plausible, because the two protomers in dimer *b* can be separated by various experimental procedures (*cf.* Madsen and Cori, 1956; Hedrick *et al.*, 1966; Kastenschmidt *et al.*, 1968a), although the forces which hold the two protomers together in the dimer are stronger than the forces which are responsible for the contact of the dimers in the tetrameric structure (*cf.* Chignell *et al.*, 1968). The substructure of dimer *b* might also be responsible in part for the 20% difference in the particle volume (V) of phosphorylase dimer *b* and the model prism. A molecular substructure

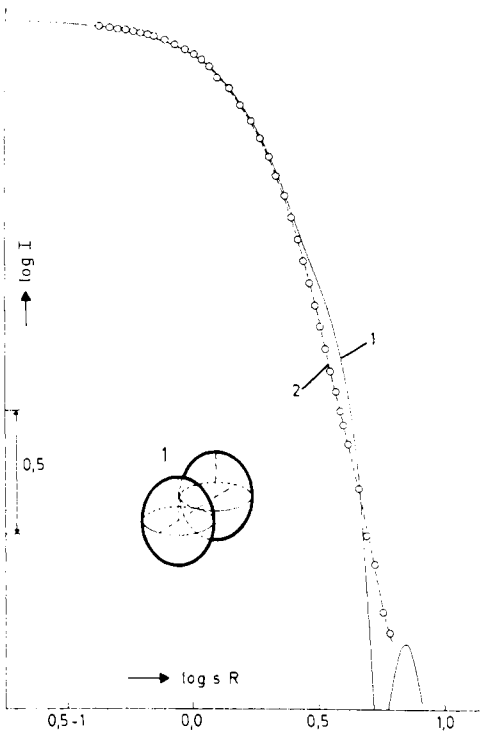

FIGURE 8: Log–log plots of the theoretical scattering curve for an ellipsoid model and of the experimental scattering curve of phosphorylase dimer *b*. Curve 1 is the theoretical curve for a model made from two ellipsoids of rotation with the axial ratio 1:1:1.18. Curve 2 is the experimental curve of dimer *b*. Conditions and symbols are those given in Figure 6.

of phosphorylase dimer *b* is also apparent from the electron microscopic pictures of Chignell *et al.* (1968), which show a groove in the middle of the dimer.

Valentine and Chignell (1968) have assigned a rhombic shape to phosphorylase tetramer *b*, which is brought about by the symmetrical association of identical dimers, each of which contains two similar but not identical monomeric subunits. Our models for phosphorylase tetramer *b* are also based on the assumption of symmetrical association of identical dimers. Unfortunately however our data give no information to either support or reject the suggestion that the monomers are not identical.

The small-angle X-ray scattering method allows to describe the forms of proteins in solution. Its limitation is that one can only indirectly deduce shape and form from a comparison with model structures which give equivalent scattering, but the actual form of the molecule cannot be directly derived from X-ray small-angle scattering as it can be done from X-ray diffraction of crystals or by electron microscopy of a fixed specimen. Additional information on the molecular structure of phosphorylase is therefore needed. Graves *et al.* (1965) found that phosphorylase *b* forms aggregates at low pH (pH 6.0) and at temperatures below 13°. The aggregated enzyme is inactive. It should be interesting to determine the form of these aggregates in order to see, for example, whether the subunits associate linearly or form some other arrangement of a higher molecular order than the tetrameric form. The methods which have been developed for the analysis of dimer–tetramer mixtures by small-angle X-ray scattering

are also applicable to mixtures of tetramers and higher aggregates. The aim of this future project is to compare inactive phosphorylase *b* with active phosphorylase *b* for which a model has been proposed in this paper. This might give some new information on the surface regions, through which the protomers make contact in regular dimeric and tetrameric forms and those contact surfaces which are involved in the formation of atypical aggregates. (See also Chignell *et al.*, 1968.)

References

Battell, M. L., Zarkadas, C. G., Smillie, L. B., and Madsen, N. B. (1968), *J. Biol. Chem. 243*, 6202.

Brown, D. H., and Cori, C. F. (1961), *Enzymes 5*, 207.

Chignell, D. A., Gratzer, W. B., and Valentine, R. C. (1968), *Biochemistry 7*, 1082.

Fischer, E. H., Hurd, S. S., Koh, P., Seery, V. L., and Teller, D. C. (1968), *in* Control of Glycogen Metabolism, Whelan, W. J., Ed., New York, N. Y., Academic, p 19.

Fischer, E. H., and Krebs, E. G. (1958), *J. Biol. Chem. 231*, 65.

Fischer, E. H., and Krebs, E. G. (1966), *Fed. Proc., Fed. Amer. Soc. Exp. Biol. 25*, 1511.

Fiske, C. H., and Subbarow, Y. (1925), *J. Biol. Chem. 66*, 375.

Graves, D. J., Sealock, R. W., and Wang, J. H. (1965), *Biochemistry 4*, 290.

Guinier, A., and Fournet, G. (1955), Small Angle Scattering of X-Rays, New York, N. Y., Wiley.

Hedrick, J. L., Shaltiel, S., and Fischer, E. H. (1966), *Biochemistry 5*, 2117.

Heine, S. (1963), *Acta Phys. Austr. 16*, 144.

Heine, S., and Roppert, J. (1962), *Acta Phys. Austr. 15*, 148.

Helmreich, E. (1969), *Compr. Biochem. 17*, 17.

Helmreich, E., and Cori, C. F. (1964), *Proc. Nat. Acad. Sci. U. S. 51*, 131.

Helmreich, E., and Cori, C. F. (1965), *Advan. Enzyme Regul. 3*, 91.

Helmreich, E., Michaelides, M. C., and Cori, C. F. (1967), *Biochemistry 6*, 3695.

Huang, Ch. Y., and Graves, D. J. (1970), *Biochemistry 9*, 660.

Illingworth, B., Jansz, H. S., Brown, D. H., and Cori, C. F. (1958), *Proc. Nat. Acad. Sci. U. S. 44*, 1180.

Kastenschmidt, L. L., Kastenschmidt, J., and Helmreich, E. (1968a), *Biochemistry 7*, 3590.

Kastenschmidt, L. L., Kastenschmidt, J., and Helmreich, E. (1968b), *Biochemistry 7*, 4543.

Kratky, Ch., and Kratky, O. (1964), *Z. Instrumentenk. 72*, 302.

Kratky, O. (1954), *Z. Elektrochem. 58*, 49.

Kratky, O. (1958), *Z. Elektrochem. 62*, 66.

Kratky, O. (1960), *Makromol. Chem. 35a*, 12.

Kratky, O. (1963), *Progr. Biophys. 13*, 105.

Kratky, O. (1964), *Z. Anal. Chem. 201*, 161.

Kratky, O., Leopold, H., and Stabinger, H. (1969), *Z. Angew. Physik. 27*, 273.

Kratky, O., Pilz, I., and Schmitz, P. J. (1966), *J. Colloid Interface Sci. 21*, 24.

Kratky, O., and Porod, G. (1948), *Acta Phys. Austr. 2*, 133.

Kratky, O., Porod, G., and Kahovec, L. (1950), *Z. Elektrochem. 55*, 53.

Kratky, O., and Skala, Z. (1958), *Z. Elektrochem. 62*, 73.

Kratky, O., and Wawra, H. (1963), *Monatsh. Chem. 94*, 981.

Krebs, E. G., and Fischer, E. H. (1962), *Advan. Enzymol. 24*, 263.

Leopold, H. (1965), *Elektronik (Germany) 14*, 359.

Madsen, N. B. (1964), *Biochem. Biophys. Res. Commun. 15*, 390.

Madsen, N. B., and Cori, C. F. (1956), *J. Biol. Chem. 223*, 1055, 1067.

Metzger, B. E., Glaser, L., and Helmreich, E. (1968), *Biochemistry 7*, 2021.

Metzger, B. E., Helmreich, E., and Glaser, L. (1967), *Proc. Nat. Acad. Sci. U. S. 57*, 994.

Mittelbach, P. (1964), *Acta Phys. Austr. 19*, 53.

Monod, J., Wyman, J., and Changeux, J.-P. (1965), *J. Mol. Biol. 12*, 88.

Pilz, I. (1969), *J. Colloid Interface Sci. 30*, 140.

Pilz, I., and Kratky, O. (1967), *J. Colloid Interface Sci. 24*, 211.

Pilz, I., Puchwein, G., Kratky, O., Herbst, M., Haager, O., Gall, W. E., and Edelman, G. M. (1970), *Biochemistry 9*, 211.

Porod, G. (1948), *Acta Phys. Austr. 2*, 255.

Porod, G. (1951), *Kolloid Z. 124*, 83.

Porod, G. (1952), *Kolloid Z. 125*, 51.

Sealock, R. W., and Graves, D. J. (1967), *Biochemistry 6*, 201.

Seery, V. L., Fischer, E. H., and Teller, D. C. (1967), *Biochemistry 6*, 3315.

Shaltiel, S., Hedrick, J. L., Pocker, A., and Fischer, E. H. (1969), *Biochemistry 12*, 5189.

Valentine, R. C., and Chignell, D. A. (1968), *Nature (London) 218*, 950.

Wang, J. H., Shonka, M. L., and Graves, D. J. (1965), *Biochemistry 4*, 2296.

Zipper, P. (1969), *Acta Phys. Austr. 30*, 143.